Molecular Motion of Isolated Linear Alkanes in Nanochannels

Johanna Becker[†]

Institut für Makromolekulare Chemie, Universität Freiburg, Stefan-Meier-Str. 31, D-79104 Freiburg, Germany

Angiolina Comotti, Roberto Simonutti, and Piero Sozzani

Department of Materials Science, University of Milano Bicocca, Via R. Cozzi 53, I-20125 Milano, Italy

Kay Saalwächter*[,‡]

Institut für Makromolekulare Chemie, Universität Freiburg, Stefan-Meier-Str. 31, D-79104 Freiburg, Germany

Received: August 25, 2005; In Final Form: October 12, 2005

The mobility of a series of linear alkanes in their inclusion compound with tris(*o*-phenylenedioxy)-spirotriphosphazene is studied by high-resolution carbon-proton magic-angle spinning solid-state NMR spectroscopy. Two different carbon-proton dipolar recoupling experiments are compared with respect to their ability to yield precise site-specific, motion-averaged dipolar coupling constants. The most accurate results are obtained by analysis of extrema positions in Lee-Goldburg cross-polarization build-up curves. We present a comprehensive collection of coupling constants, which evidence a rotational motion of the all-trans chains around the channel axis, with some further averaging due to additional fluctuations, as previously found for alkanes in other host matrices such as urea. The order parameter increases toward the inner parts of the chains, and is largely independent of chain length. Notably, chains in a TPP host are not more ordered than in urea, even though the average TPP channel diameter is reported to be smaller. Significantly decreased order is found for highly filled short-alkane samples, which is interpreted in terms of an increased rate of mutual collisions. From residual dipolar couplings as well as carbon chemical shifts, we derive similar amounts of gauche conformers. Translational motions along the channels are further studied by proton double-quantum spectroscopy, which probes guest−host dipolar couplings. The extent of local-scale lateral motion is again correlated with the sample filling, and is a weak function of temperature, as expected from a case in which highly restricted single-file diffusion should dominate the mobility. Characteristic effects of sample aging are apparent in all our experiments.

I. Introduction

Inclusion compounds (ICs) of linear organic molecules or polymers with organic channel-forming hosts such as urea, perhydrotriphenylene, or cyclodextrins, have received considerable attention during the past decades, as they represent unique model systems for the confinement of guest molecules in ordered and well-defined environments.[1] Early, extensive work on channel structures formed by urea as a host for aliphatic compounds was carried out by Schlenk.[2] Later, White has reported on the stereoregular polymerization of monomers within such inclusion compounds,[3] from which highly crystalline polymers can be precipitated by dissolution of the host. Polymer-ICs can further be formed from polymers themselves, and coalescence of the chains from these highly ordered structures can result in samples with unusual morphologies or specific crystal structures.[4,5]

Another interesting aspect of such ICs is that they represent model systems for the study of the dynamics of isolated chain molecules. As the interactions between polymer and channel are usually of minor importance, it becomes possible to study motions of the individual segments being primarily influenced by local conformational barriers within the chain and the topology of the channel constraint.[6] Such information should be useful to ultimately unravel the complex interplay of inter- and intrachain constraints for the segmental motion in polymeric melts. Guest dynamics in inclusion compounds has been studied for some time now, and solid-state NMR plays a dominant role in this regard,[7−20] as it offers direct, site-specific information on amplitude and time scale of the motional processes.[21]

Most of the previous results have been obtained by deuteron NMR,[7,8,13−17] where in different matrices, changes in the line shape usually indicate a relatively sharp transition from a rigid phase considerably below ambient temperature to a phase in which fast three-site jumps or rotations of the included molecules about the channel axis occur. Specifically, the "rotation" of an all-trans alkane chain leads to an averaging of the CD_2 quadrupolar tensor by a factor of 0.5, and lower values indicate the presence of additional librations, and more importantly, a population of gauche conformations.[16] These interpretations can be corroborated by observations of isotropic ^{13}C chemical shifts, which depend on conformation[22] and which change with the length of the included alkane.[9]

Deuterium NMR suffers from the need for specifically labeled guest molecules. Imashiro et al.[10] have published an early attempt to circumvent this limitation by exploiting the site-

* Corresponding author. E-mail: kay.saalwaechter@physik.uni-halle.de.
[†] Now at Forschungsinstitut für Molekulare Pharmakologie, Robert-Rössle-Str. 10, D-13125 Berlin-Buch, Germany.
[‡] Current address: Fachbereich Physik, Martin-Luther-Universität Halle-Wittenberg, Friedemann-Bach-Platz 6, D-06108 Halle, Germany.

10.1021/jp054795d CCC: $30.25
Published on Web 11/19/2005

resolution provided by the ^{13}C chemical shift. Dipolar switched-angle sample spinning (SASS,[23]) was applied on ICs of C_7H_{16} to $C_{10}H_{22}$ in urea to determine motionally averaged $^{13}C-^{1}H$ heteronuclear dipolar coupling constants, which basically provide the same information as quadrupolar splittings in ^{2}H NMR. Their results did not show the clear trend concerning the chain length dependence which is observed for the isotropic ^{13}C shifts[9] and quadrupole splittings[16] in these compounds, indicating that the accuracy of this experimentally challenging method is limited.

In the meantime, new, powerful, and more robust magic-angle spinning (MAS) methods have been developed to accurately measure heteronuclear (as well as homonuclear) dipolar coupling constants,[24−28] and some of these have already been applied to the study of the chain dynamics of poly(dimethylsiloxane) in its inclusion compound with γ-cyclodextrin.[19] We here present a comprehensive study of chain-length effects on the motional amplitude of all individual resolvable groups of alkane chains included in the aromatic nanochannels of tris(*o*-phenylenedioxy)spirotriphosphazene (TPP). This host material offers channels of about 4.5 Å diameter,[29] which are somewhat narrower than the ones in urea (5.25 Å). We compare our findings with the chain-length dependent chemical shift reported earlier,[18,20] as well as with measurements of alkanes in urea, for which accurate ^{2}H data exist in the literature.[16,17] In addition, we report systematic observations of guest−host dipolar contacts using ^{1}H homonuclear double-quantum spectroscopy, which for the first time allow us to draw conclusions on the extent of lateral alkane motion within such channels.[19]

II. Experimental Section

Samples. We have investigated ICs of TPP with linear, saturated alkanes: C_7, C_9, C_{12}, C_{16}, C_{24}, C_{36}, and C_{54}, which are referred to as TPP−C*n*. The TPP and its ICs were prepared following the procedures of Allcock,[29] which are also outlined in our previous work.[18] As a comparison, we have investigated the ICs of $C_{12}H_{34}$ and $C_{16}H_{34}$ with urea (urea-C*n*), which were prepared by precipitation from a concentrated solution of urea in methanol.[2,17] The identity and overall purity of the compounds were checked by DSC and X-ray diffraction. The investigated TPP ICs fall into two classes: some samples were about 1 year old at the time of investigation and exhibited small amounts of impurities at or below the 10% level, while all other samples were fresh and virtually contaminant-free. The former are denoted by TPP−C*n*i (initial samples with impurities).

ICs of short-chain alkanes vary somewhat in their stoichiometry, and for a closer inspection of related effects, one sample of TPP−C7 was evacuated to 10 mbar at 348 K for 2 and 6 h to yield TPP−C7r1 and TPP−C7r2, respectively, in which the alkane filling factors were reduced by about 10% and 22%, respectively. Filling factors were determined by integration of ^{1}H MAS spectra. As is known from previous experiments,[30] evacuation of the channel structure under the conditions we have used to prepare TPP−C7r1 and −C7r2 is well possible without affecting the integrity of the compound. In fact, the empty TPP channels were in the cited work re-filled with laser-polarized ^{129}Xe in order to investigate the long-time characteristics of single-file diffusion, which necessitates intact channels.

Impurities in the samples comprise nonincluded alkanes and possible degradation products of TPP, visible as weak additional signals in the spectra (see Figure 1b). Nonincluded alkane contaminants can easily be identified by the appearance of additional methylene signals, as the included alkane carbon and proton resonances are shifted upfield by about 1.4 and 2.2 ppm, respectively, as a result of ring-current effects of the TPP.[20] Such impurities are most often not observable in CP-MAS experiments, as they are liquid-like. The only problematic case is TPP−C54, where the nonincluded part is solid at room temperature, but appears sufficiently separated from the main resonance. Its overlap with the β-methylene resonance is inconsequential as the latter would be too weak to be analyzed. Generally, the unique ring current-induced chemical shift of included alkane signals ensures that the data are representative for locally intact channel structures. All samples were studied at natural isotopic abundance.

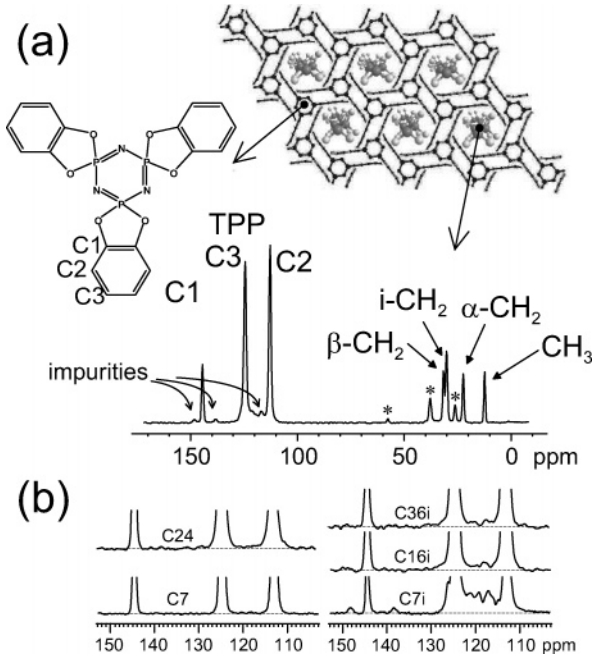

Figure 1. ^{13}C CP MAS spectrum of TPP−C9i, along with assignments and structures (a). Expanded views of the aromatic regions of different compounds show the impurities (b).

NMR Spectroscopy. Experiments were carried out on a Bruker Avance 500 spectrometer (B_0 = 11.7 T). The sample temperature, which depends on the MAS frequency due to rotor friction, was controlled according to known calibration procedures[31] and amounted to 303 K unless specified otherwise. The recycle delay was 2 s in all cases. CH dipolar coupling constants (D_{CH}) were determined by fits to spinning sidebands created by the rotor-encoding REDOR (REREDOR) method,[28,32] as well as by Lee−Goldburg cross polarization (LG-CP) build-up.[26] ^{13}C chemical shifts were externally referenced against the methylene signal of adamantane at 29.5 ppm, which corresponds to a crystallite signal of high-density poly(ethylene) at 32.96 ppm. The best internal reference of the TPP−ICs is the sharp aromatic C1 carbon signal at 144.7 ppm (see Figure 1a).

REREDOR experiments rely on fast (25−30 kHz) MAS in a Bruker 2.5 mm double-resonance probe, where rf pulses and TPPM decoupling[33] were applied at 125 kHz (2 μs 90° pulses). Ramped CP was employed to create initial ^{13}C magnetization,[34] 40 t_1 increments were acquired over two rotor periods for rotor-encoding, slices along t_1 were then duplicated several times, damped, and Fourier transformed to obtain sideband patterns. Using two rotor periods, it is ensured that signals representing the noise level appear at noninteger sideband positions in the patterns.[27] A rising ramp was applied with a 20% variation around an average proton rf frequency of about 60 kHz, while the carbon frequency was always centered on the −1 MAS sideband match, $\omega_{1C} = \omega_{1H} - \omega_R$.

LG-CP experiments were performed in a 4 mm MAS probe at a pulse and decoupling frequency of 83.3 kHz (3 μs 90° pulses), and with 10.9 kHz spinning, which avoids an overlap of aliphatic signals and aromatic spinning sidebands. The LG-CP contact was realized without a ramp at a constant $\omega_{1H}/2\pi = 60$ kHz and a frequency offset of +42.5 kHz, with the carbon frequency again optimized at the −1 sideband condition. The influence of instrumental drift was checked and reduced by co-adding the signals from several sequentially acquired full 2D protocols for the intensity build-up. The setup quality and drift effects can sensitively be monitored by aid of the aromatic resonances of TPP; see below for further details.

^{1}H fast-MAS 1D and 2D double-quantum (DQ) MAS spectra were also acquired with the 2.5 mm probe at 30 kHz spinning. This experiment probes the proximity of protons in terms of through-space homonuclear dipolar couplings, and it is the solid-state analogue of the INADEQUATE experiment known from solution-state NMR.[35] In the present context, signal intensities corresponding to dipolar contacts between alkane and host protons are dependent on the averaging of their coupling due to motion along the channel. For these experiments, the back-to-back (BaBa) pulse sequence[36] was used, where the compensated version[37] was applied in experiments with excitation times equal to an integer multiple of four rotor cycles ($n \times 133$ μs).

Data Analysis and Simulations. Spin dynamics simulations of the explicit pulse sequences with finite pulses were performed with a home-written code performing a numerical stepwise integration of the Liouville−von-Neumann equation of motion using a product-basis representation of the density matrix. The program is in many respects similar to the publicly available SIMPSON package.[38] Powder averaging was in all cases performed using the REPULSION scheme with 384 polar orientations evenly distributed over a sphere,[39] and up to 21 γ angles (rotor phase). The local geometry of the simulated all-trans alkanes was taken to be tetrahedral, with C−C and C−H bond lengths of 1.53 and 1.09 Å, respectively ($\Rightarrow D_{CH}/2\pi = 23.1$ kHz). We define the backbone order parameter of an all-trans alkane rotating around its long axis as

$$S_b = \frac{2D_{res}}{D_{stat}} \quad (1)$$

with D_{res} as the residual coupling constant. The factor 2 arises from the 90° angle between the C−H bond and the rotation axis. Given the coordinates of the simulated spins, the rotation (equivalent to a symmetric three-site jump) is explicitly performed by the software and results in dipolar tensors which are collinear with the rotation axis. The symmetry then being uniaxial, averaging effects beyond a simple rotation (e.g., librations, contributions of gauche conformations) can be included in terms of S_b as a scaling factor for all couplings. Experimentally, $D_{stat}/2\pi = 21.5$ kHz is taken from a LG-CP reference experiment on high-density polyethylene (crystallite signal). This value was found to be temperature-independent within 300 Hz between ambient temperature and 353 K, and its use should correct for the influences of fast bond vibrations, assuming that these do not depend much on the molecular packing and additional dynamics on longer time scales.

III. Results and Discussion

Figure 1a shows the ^{13}C CP MAS spectrum of TPP−C9i along with a sketch of its channel-like structure (seen from above) and an assignment of the signals. Note the small amount of contaminants visible in the aromatic region. For the included

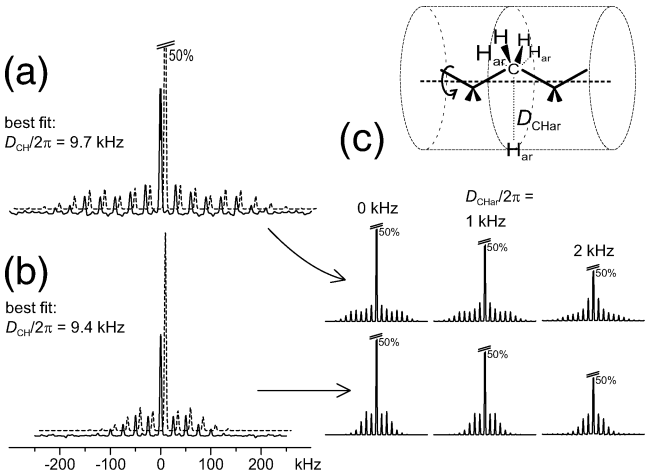

Figure 2. REREDOR sideband patterns detected at the i-CH_2 carbon resonance of TPP−C9i, acquired at 30 kHz MAS and four rotor periods recoupling (a) and 25 kHz MAS with two rotor periods recoupling (b), corresponding to encoding times of 133.3 and 80 μs, respectively. Best fits are shown as dashed lines. Part (c) shows results of spin dynamics simulations, which are further described in the text.

alkanes, it was generally possible to determine distinct chemical shifts and dipolar couplings for the CH_3 as well as the α-, β-, and inner (i-) CH_2 resonances. The latter always gave rise to a single peak. The level of impurities in the TPP−C*n*i series decreases with increasing chain length, as can be seen in Figure 1b.

A. REREDOR Sidebands: Isolated Methylene Approximation. REREDOR represents a simple and easy-to-use alternative to traditional separated local-field (SLF) experiments[40] for the determination of heteronuclear dipolar coupling constants under MAS.[28] The method is here mainly used to investigate the possibility of treating the methylene groups as isolated moieties, as rotating methylene groups represent unique properties in SLF experiments (see below). In REREDOR, the proton homonuclear decoupling is left to fast MAS in excess of 25 kHz alone, and under these conditions, it was shown that indeed, data analysis can be done under complete neglect of homonuclear couplings.[27] The experiment basically consists of two REDOR-type recoupling periods used for rotor encoding, separated by the t_1 evolution period, the main function of which is to allow for a change in the rotor phase effective during the second encoding period. This leads to a t_1-dependent intensity modulation detected at the different ^{13}C resonances, which results in a characteristic spinning sideband pattern after Fourier transformation.

Sideband patters recorded using different recoupling times at different MAS frequencies are shown in Figure 2a and b. They can be fitted to the Fourier transformation of the powder-averaged time domain signal given by[28]

$$I \propto \langle \prod_i \cos(\Phi^{(i)}_{enc1} - \Phi^{(i)}_{enc2}) \rangle$$
$$= \left\langle \left[\frac{1}{2} + \frac{1}{2}\cos(4\Phi_{enc1} - 4\Phi_{enc2}) \right] \times \cos_{ext} \right\rangle \quad (2)$$

where $\Phi^{(i)}_{enc1,2}$ is the phase associated with the *i*th proton coupled to the detected carbon acquired under heteronuclear dipolar recoupling during the first or second encoding period and is proportional to the dipolar coupling constant. For simplicity, we have here neglected the small correction due to dipolar evolution during t_1.[28] The second line of eq 2 embodies a simple trigonometric transformation of a $\cos^2$ term, which

arises because the two CH dipolar tensors within a methylene group rotating rapidly about an axis within its symmetry plane are exactly equal ($\Phi_{enc}^{(1)} = \Phi_{enc}^{(2)} = \Phi_{enc}$). $\cos_{ext}$ comprises a product over all other cosine contributions from external perturbing spins. This term was neglected in the fits, and the strong centerband was also excluded. Note that perturbations arising from the nearest-neighbor in-chain protons are negligible in rotating all-trans chains, as the orientation of the corresponding coupling tensors is close to the magic angle, leaving guest−host contacts as the dominant factor.

The applicability of the addition theorem and the appearance of the two contributions has a direct quantum-mechanical correspondence[23] and is a peculiarity of SLF spectra of rotating methylene groups: the constant term 1/2 in eq 2 corresponds to methylene groups in which the carbon is coupled to two protons with opposite spin states, and the effective coupling cancels when the interaction tensors are identical. The second term is rotor-modulated by effectively twice the coupling constant, as the phases add up when the protons have equal spin states (another factor of 2 enters through the addition theorem). The unmodulated contribution, which in Fourier space leads to a sharp central line containing half the signal, offers the possibility to monitor the external perturbations described by the $\cos_{ext}$ term. These modulations lead to additional spinning sidebands, thus reducing the centerband. As is obvious from Figure 2a and b, the characteristic centerbands are reduced by about 50% when comparing the experimental results to the fits.

To investigate the level of perturbation, Figure 2c shows results from simulations using $D_{res}/2\pi = 9.4$ kHz, in which potential perturbations by the aromatic host were modeled with three additional, symmetrically placed protons with effective coupling constants denoted as $D_{CHar}/2\pi$. The model was chosen so as to represent the cylindrical symmetry of the perturbative local field with a minimum number of spins (simulations with more than eight spins are hardly feasible). 50% reductions of the centerband are indeed observed for perturbing couplings on the order of 2 kHz. The outer sideband manifold is not changed considerably for perturbations of 1 kHz, while the relative increase of the ±1 and ±2 sidebands at 2 kHz is not in agreement with the experimental manifolds, which are well represented by the nonperturbed solution. This gives us a qualitative picture for the level of perturbation, where the value of 1−2 kHz should be regarded as a second moment comprising the action of many rather weak couplings, which are, of course, averaged by translational back and forth motions along the channels (see section III.D).

As to sensitivity, REREDOR was not suited to detect significant differences between the different TPP−C*n* samples, as the accuracy of the dipolar couplings was no better than 5% after experimental times in excess of 24 h. This is mainly due to the low filling factor of the alkanes, which are diluted in the host matrix, and the low signal from the 10−15 mg filling of a 2.5 mm rotor. Better conditions are provided by 4 mm rotors and slower MAS, where the increased signal enabled us to determine dipolar couplings with much improved accuracy.

B. LG-CP Build-up Analysis: Precise CH Dipolar Couplings. At MAS frequencies much below 20 kHz, homonuclear decoupling by rf pulses is essential but is often difficult to control precisely due to setup-specific scaling factors. The difficulties of Imashiro et al. to obtain conclusive results may here serve as an illustration.[10] As an alternative to traditional slow-MAS SLF experiments employing homodecoupling, we have tested the robust and simple LG-CP experiment proposed by van Rossum et al.,[26] which was also previously used for the study of molecular dynamics.[41] It combines the simplicity of CP build-up analysis with the even more simple and robust homodecoupling afforded by switching the proton carrier frequency off-resonance during CP, such that the effective quantization axis is at the magic angle with respect to B_0.[42] Effects of rf imperfections are minor, as the off-resonance irradition is used only for spin-locking rather than evolution around its symmetry axis.

LG-CP build-up curves depend less specifically on the topology of the local dipolar field than on REREDOR sidebands, as it is not an SLF experiment in the classical sense.[23] For instance, the spins associated with the "central transition" of an isolated CH_2 group do not contribute to the build-up, while they do contribute to a rather slowly increasing contribution when remote couplings are present (see below). We chose to take an approach to data analysis that differs from the one proposed in the original work. Van Rossum et al. have acquired build-up data in small steps, starting from $\tau_{LGCP} = 0$ to rather high values, which is a lengthy procedure when many scans are to be acquired at natural abundance. They then performed a Fourier transformation to obtain dipolar line shapes, from which a characteristic frequency splitting was determined and compared with simulated results.

A time-saving alternative is to focus on the position of one of the extrema in a build-up curve. As a starting point for the analysis of experimental data, we have performed simulations of isolated CH_2 and CH_3 moieties and determined the positions of the different extrema. In the original publication,[26] a linear relationship between the frequency splitting and the dipolar coupling of an isolated CH pair was found. Therefore, we have plotted the dipolar coupling used in the simulations vs the inverse τ_{LGCP} for different extrema positions, see Figure 3a, and fitted these data to

$$D_{res}/2\pi = a1/\tau_{LGCP} + a2/\tau_{LGCP}^{2} \qquad (3)$$

The results of the fits can be found in Table 1 and should be of future use. In the case of rotating CH_2 and CH_3 units, linearity is roughly obeyed, with only weak quadratic corrections. The quadratic term is significant when a rigid CH_2 is considered. This is not surprising, as the corresponding dipolar spectra do not exhibit the single splitting characteristic for CH pairs[26] or rotating methylene groups,[41] but have a more complex shape. Here, we have performed 7-spin simulations in order to account for the influence of neighboring in-chain protons, see the sketch in Figure 3a. Note again that in a rotating all-trans chain, the associated couplings vanish due to the magic-angle orientation of the respective tensors. The rigid-CH_2 calibration data were actually used to determine the static reference coupling of rigid all-trans chains in HDPE crystallites. For the rotating CH_3, the orientation was chosen in accordance with an all-trans chain terminus; note the additional reduction factor of 1/3 due to methyl rotation.

Experimental LGCP build-up data are shown in Figure 3b, where they are compared with simulated results. For most other measurements, we chose to acquire spectra only between $\tau_{LGCP} = 100$ and 740 μs, with an increment of 10 μs, covering the first two maxima for CH_2 and the first maximum for the CH_3 group. Polynomial interpolation was used to locate the second and first maximum in either case, respectively, and dipolar couplings were then obtained from eq 3. In this way, we were able to determine CH couplings with an average accuracy of 1% (about 100 Hz) within 9 h experimental time, based on statistical deviations among different experiments. The accuracy was notably lower for the very weak chain-end signals of the

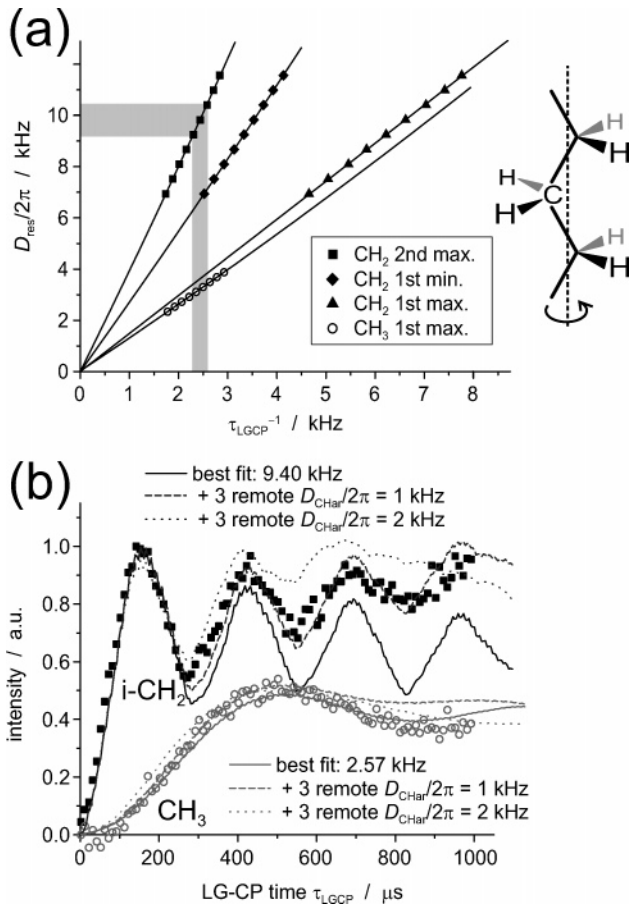

Figure 3. Plot of residual couplings of rotating CH_2 and CH_3 groups vs simulated reciprocal extrema positions (a), and LG-CP intensity build-up data for TPP-C9i along with simulated build-up curves, matched to the best-fit CH residual dipolar couplings determined from the maxima of the curves (b). The fits shown in (a) as solid lines were used to determine couplings from experimental build-up data, and the shaded region indicates the range of experimental data for the i-CH_2.

TABLE 1: Parameters for LG-CP Data Analysis Using eq 3, which Was Fitted to Extremum Positions in Simulated Build-up Curves for Different Functional Groups

moiety	extremum	a1	a2/ms
rot. CH_2	first max.	1.486	0
rot. CH_2	first min..	2.680	0.0294
rot. CH_2	second max.	3.870	0.0676
rot. CH_3	first max.	1.272	0.0150
rigid CH_2	second max.	0.953	0.874

longer alkanes, and more so for the CH_3 units, for which the location of the rather broad maximum is additionally challenged by noise.

As is indicated by the simulation results, including three remote channel protons (see Figure 2a for a sketch of the geometry), the positions of the first two maxima are hardly affected by long-range couplings, but the long-time behavior is represented more accurately. In accordance with the literature,[26] the remote couplings mainly lead to an additional slowly increasing intensity contribution that corresponds to the observation of a central line in the dipolar spectrum.

To estimate the influence of experimental imperfections, we have checked the effect of carrier frequency offsets and deviations from the ideal rf nutation frequency (power level) on the two channels, which both affect the −1 sideband matching (=recoupling) condition as well as the LG condition in the case of protons. Generally, the extremum positions tend to shorter τ_{LGCP} when offset, rf frequencies shift away from ideality in either direction, and the functional dependencies appear parabolic. Deviations up to ± 2 kHz are tolerable when the results for the couplings should not be systematically overestimated by more than 2%. When one of the frequencies deviates already by about 5 kHz, an additional ±1 kHz change shifts the extrema by about 10 μs. This sensitivity can be utilized as a test criterion: as the matching condition was optimized for the aliphatic resonances, we always checked the position of the second maximum of the rigid TPP C2-resonance at 113 ppm (about 10 kHz off), which under our conditions was always found within $\tau_{LGCP} = 240 \pm 10$ μs.

TABLE 2: Filling Factors and Site-Specific Residual Dipolar Coupling Constants $D_{res}/2\pi$ Determined by LG-CP Build-up Analysis for the Various Samples

sample	filling[a]	*i*-CH_2	*β*-CH_2	α-CH_2	CH_3
TPP−C7	3.71	9.53	9.21	8.27	3.38
TPP−C7	3.38	9.74	9.58	8.66	3.11
TPP−C7	3.16	9.79	9.39	8.91	3.63
TPP−C7r1	2.84	9.91	9.73	9.07	3.32
TPP−C7r2	2.45	9.92	9.71	9.14	3.06
TPP−C7i[b]	1.09	9.17	8.96	8.23	2.41
TPP−C9	3.76	9.72	9.28	8.37	3.20
TPP−C9i[b]	2.18	9.40	9.14	8.04	2.57
TPP−C12	3.05	10.4	10.2	9.39	4.29
TPP−C12i[b]	3.27	9.65	9.44	8.33	2.63
TPP−C12ht[c]	3.27	9.31	9.22	7.73	2.86
TPP−C16	3.60	10.4	9.62	8.81	3.85
TPP−C16i[b]	3.49	9.78	9.63	8.12	2.45
TPP−C24	3.55	10.30		8.59	2.87
TPP−C36i[b]	3.55	10.22		8.44	2.64
TPP−C54	3.55	10.42			
TPP−C54ht[c]	3.55	10.16			
urea-C12	1.44	10.24			
urea-C16	1.36	10.56			

[a] The filling is given in terms of CH_2 units per TPP (or urea) molecule, and coupling constants are in kHz. [b] Samples with impurities. [c] High-temperature experiments at 343 K.

C. Discussion and Comparison with Previous Results. All site-specific residual dipolar couplings obtained from LG-CP build-up analyses are collected in Table 2 and plotted vs the alkane chain length in Figure 4a. In this and the following graphs, data for the aged samples are always identified by crosses. As a first major observation, we note that the mobility of the different groups increases toward the chain ends, which can be intuitively expected. As to chain-length effects, there is a significant tendency toward reduced i-CH_2 and *β*-CH_2 couplings for shorter chains in some of the samples, in particular the aged ones. These findings will be further discussed below. The CH_3 and α-CH_2 couplings exhibit no significant trends beyond their larger statistical scatter.

The temperature dependence was checked in two cases (see Table 2) and was found to be minor: heating by 40 K results in an average reduction of all residual couplings by 4%, which we interpret as a slight increase in the average amount of gauche conformations, over which the chain motion averages in the fast limit. Fast-limit averaging is basically indicated by the observation of well-defined REREDOR sideband spectra (Figure 2) and LG-CP build-up curves (Figure 3).

Upon application of eq 1, backbone order parameters can be calculated and compared with previous literature experiments on ICs of TPP and urea, see Figure 4b. To render the cited data comparable, we reference the reported SASS values of urea-ICs to our experimental D_{stat} measured on HDPE instead of using the theoretical value calculated from internuclear distance and motional geometry, where the result would be underestimated due to the neglect of fast bond librations.[10] We proceed

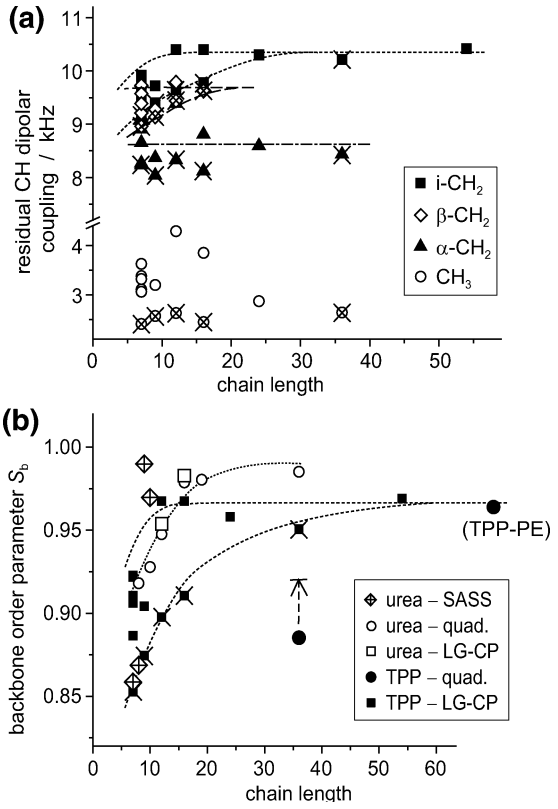

Figure 4. Residual CH dipolar couplings (a), and backbone order parameters (eq 1) for the inner parts of the chains (b), plotted vs the alkane chain length. All lines are merely guides to the eye, and crossed symbols denote the samples with impurities. In (b), the ambient-temperature order parameters determined in this work are compared with literature data: SASS of urea-ICs;[10] ^{2}H quadrupole splittings of urea-ICs;[16,17] quadrupole splittings in TPP−ICs.[43] The arrow in (b) indicates a correction due to the reported splitting being an average over the whole C36 chain.

analogously with the ^{2}H quadrupole splitting data of urea-ICs by the Volds and co-workers[16] and of TPP−ICs by Simonutti et al.,[43] where we use the experimental quadrupole splitting observed for PE crystallites, $\Delta\nu_{Q,\mathrm{stat}} = 122$ kHz,[44] thus ensuring a comparison of the two different methods on the same footing.

Our LG-CP data for urea-ICs (open squares) agree very well with the literature data (open circles), which proves the validity of our approach. Yet, the SASS data deviates rather dramatically in both directions and much beyond the stated error interval of 0.03,[10] which we ascribe to the instrumental challenges posed by this method or to problems related to the sample preparation. Our TPP−C*n* data extrapolates well to the ^{2}H-based value of TPP−PE, yet the agreement is less good for TPP−C36. This is basically due to the rather significant line broadening observed in the preliminary report of Simonutti et al.,[43] and its origin remains to be investigated. A relationship with sample aging effects (see below) appears possible. The methylene splittings at the ends of the fully labeled chains could thus not be distinguished, as was possible for the case of urea-C*n*. The reported quadrupolar couplings are therefore an average over the α-, *β*-, and i-CH_2 groups. A simplistic weighted average over corresponding experimental and expected dipolar values (Table 2) yields $S_b \approx 0.92$, thus explaining part of the deviation (see the arrow in Figure 4b).

On the whole, the data in Figure 4b convincingly demonstrate that the molecular order of alkane chains in TPP is only about as high if not lower than in urea. This is surprising, considering that urea offers channels with a significantly larger average van der Waals diameter (5.25 Å, as opposed to 4.5 Å). This shows that topological details, and possibly also specific dispersion interactions (aromatic environment vs N- and O-centered lone pairs) play a role. This should be the focus of future computer simulations.

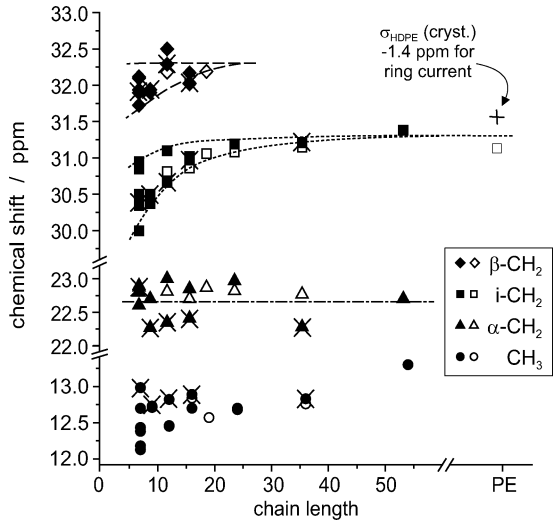

Figure 5. ^{13}C chemical shifts of the alkane resonances in the TPP−ICs as a function of chain length. Open symbols correspond to literature data,[18] which was shifted by 1 ppm in order to account for the use of different shift references. Crossed symbols again denote aged samples.

Figure 5 presents our experimental ^{13}C chemical shift data and another comparison with literature data.[18] The general observation is a significant similarity of the observed trends to the dipolar data of Figure 4, the absolute scale shift of course being primarily influenced by chemical details. Again, the chain-end signals exhibit no marked trend and will thus not be discussed further, while the shifts of the i-CH_2 tend to lower values for most samples with shorter alkanes. Chain-length dependent chemical shifts have earlier been observed for the case of urea-ICs[9] and have been ascribed to a rapid averaging process involving a small fraction of gauche conformations, where the well-known *γ*-gauche effect[22] should dominate the observed trend.

In Figure 6 we collect data providing a rationale for the large scatter of dipolar couplings as well as chemical shifts toward shorter alkane chains. It is increasingly difficult to prepare ICs of shorter, volatile alkanes which exhibit the maximum stoichiometry of about 3.6 CH_2 units per TPP molecule (Figure 6a). Our collection of TPP−C7 ICs with different fillings serves to explain the trends observed for residual couplings as well as chemical shifts of the inner methylenes. Both quantities are plotted in Figure 6b vs the filling, and we observe a significant decrease of both quantities toward higher fillings. The same trend is in fact found for the couplings associated with the *β*- and α-methylenes, see Table 2. This suggests that shorter alkane−alkane distances lead to increased amounts of gauche conformations, even in the inner parts of the chains. This represents in our view a nice piece of experimental evidence in support of the travelling defect model, which was promoted frequently in earlier work.[12,14] Here, gauche defects might be introduced by more frequent alkane−alkane collisions at high filling.

Note that this model also provides a natural explanation as to why a very long PE chain can also perform apparent rotations. Rather than relying on the rather unrealistic assumption of a rigid-body rotation of a whole chain subject to added friction, low-energy defects would be responsible for the overall rotation

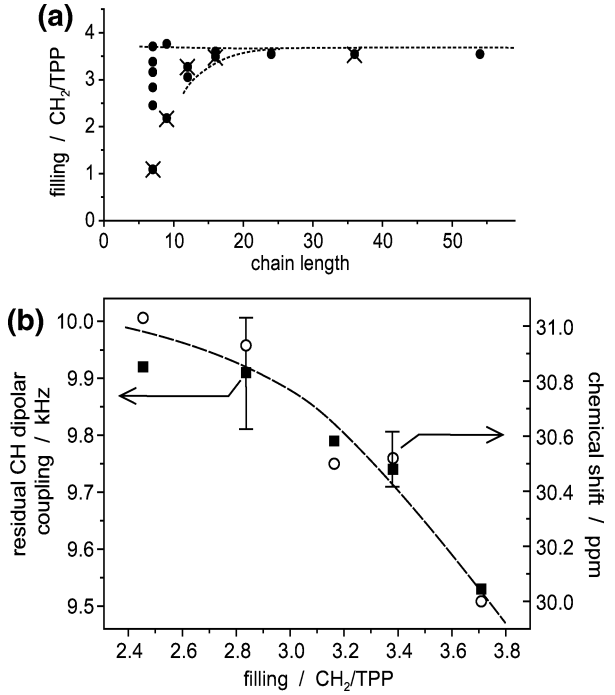

Figure 6. Stoichiometry of the TPP ICs in terms of the filling with CH_2 units per TPP molecule as a function of chain length (a), and residual dipolar couplings as well as chemical shifts of the γ-CH_2 group in the different TPP−C7 compounds as a function of filling (b). Crossed symbols in (a) again denote aged samples, and the line in (b) is a guide to the eye.

of the segments. Note that the energy associated with gauche−trans conformational isomerizations of methylene units in PE is estimated to be around 14.7 kJ/mol, while T_1 relaxation data of PE confined to perhydrotriphenylene channels indicated an apparent activation energy for chain rotation of about 4.6 kJ/mol.[12] Therefore, the specific environment of IC channels might facilitate conformational jumps by providing a different energetic stabilization of the conformers, and this might also explain why molecular order in TPP is lower than in urea. Defects made up of small-angle twists extending over about 10 methylene units were also discussed as a probable cause of rotation, and such "twiston" states[45] could also catalyze conformational jumps.

The finding of decreased order at higher fillings is corroborated by a very recent paper, in which chain compression in urea-ICs, afforded by externally applied Helium pressure, was found to result in an increase of the gauche fraction at the chain ends.[46] The data in Table 2 confirms that the effect in TPP−C7 is indeed more pronounced at the chain in ends, where the decrease of order detected at the α-CH_2 is about 10%, while 4% is the range observed for the inner (γ) methylenes. In summary, we hypothesize that unloading results in less vigorous interalkane collisions and a consequently reduced induction of gauche defects.

Note that this explanation does not hold for the aged samples, which exhibit low dipolar couplings despite their low filling. We might speculate that the impurities are located in otherwise empty channels, and push the remaining alkanes into the remaining intact parts of the structure, where the effective filling is high. This is corroborated by the fast-MAS results to be presented in the next section.

Having already alluded to a fraction of gauche conformers as the reason for lower residual dipolar couplings and chemical shifts, we proceeded by analyzing both types of data in terms of such a fraction f_{gauche} using two very simple models: As to

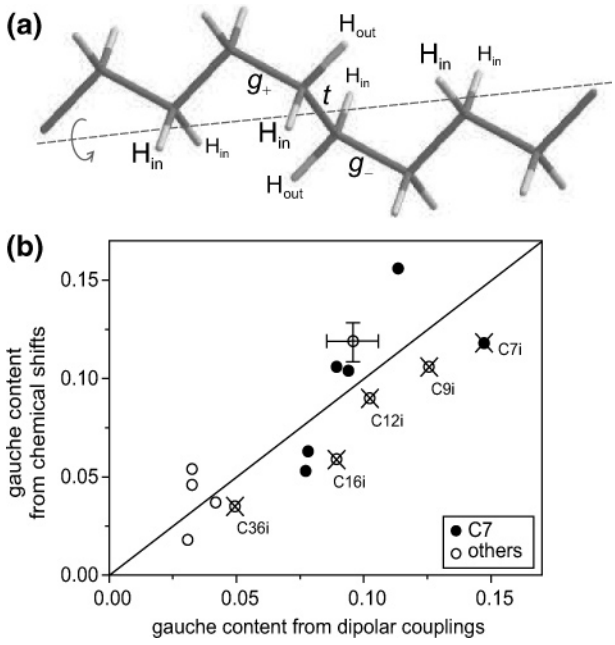

Figure 7. A chain with a typical kink defect (a), and comparison of the fractions of gauche conformers in the different TPP ICs as calculated from dipolar couplings (eq 4) and chemical shifts (eq 6). The line has a unity slope, and crossed symbols again denote aged samples.

dipolar couplings, we first note that in channels of about 4.5 Å diameter, only three different types of conformers, i.e., the all-trans chain and two symmetry-related $\{g_+ - t - g_-\}$ conformers need to be considered.[6] The latter correspond to chains with a simple kink defect, see Figure 7a. Following the arguments given by Cannarozzi et al.,[16] we assume that only the dipolar tensors within the two methylenes adjacent to the central trans bond attain notably different orientations when compared with the extended chain. One of the protons is oriented within the original methylene plane ("H_{in}"), while the other points away from this plane along the original chain direction ("H_{out}"). Rotational averaging leads to reductions of the respective dipolar tensors by the familiar factor of $P_2(\cos 90°) = -(1/2)$ in the former case, while $P_2(\cos 35.25°) = +(1/2)$ results for the latter.

Upon fast-limit averaging among the two different types of protons (each methylene group is on average involved in the same number of g_+ and g_- conformations), the mean dipolar coupling associated with CH_2 groups in gauche conformations is therefore seen to be zero. The experimental chain order parameter given by eq 1 is therefore obtained as $S_b = S_{ideal}(1 - f_{gauche})$, and the final result is simply

$$f_{gauche} = 1 - S_b \tag{4}$$

because $S_{ideal} = 1$ by definition, see eq 1.

As to the chemical shifts of the inner methylenes, we assume a γ-gauche effect of $\Delta\sigma = -5$ ppm[22] for those units for which the CH_2 (or CH_3) moiety in γ position attaints a spatial proximity when the central bond between them is in a gauche conformation. Neglecting chain-end effects, the fast-limit averaged chemical shift is therefore

$$\sigma = \sigma_0 + 2f_{gauche}\,\Delta\sigma \tag{5}$$

where the factor of 2 arises from the two possible neighbors. We use $\sigma_0 = 32.96$ ppm − 1.4 ppm = 31.56 ppm as the (estimated) chemical shift of a PE chain in a TPP environment with a −1.4 ppm shift due to ring currents,[20] and therefore obtain

$$f_{\text{gauche}} = \frac{31.56 \text{ ppm} - \sigma}{10 \text{ ppm}} \quad (6)$$

Note that this treatment must be taken with a grain of salt when the rather short alkanes are considered, because a specific carbon shift is mostly affected by the conformation at the next but one bond. For example, the chemical shift of the single, central γ-CH_2 in TPP−C7 is mainly determined by the average bond conformations between the β and the α methylenes, while its residual coupling is mostly affected by the directly adjacent bond comformations.

The results of these analyses can be inspected in Figure 7b, where the gauche contents calculated on the basis of these rather simple models are seen to be well correlated within our range of experimental accuracy. Interestingly, the aged samples deviate systematically toward increased dipolar couplings or increased chemical shifts (which results in apparently reduced gauche contents).

D. Double-Quantum Correlation Experiments: Lateral Mobility. Using 2D homo- and heteronuclear correlation methods, we have previously observed explicit dipolar contacts between mobile guests and the rigid matrix in the special cases of polymers such as poly(dimethylsiloxane) included in γ-cyclodextrin[19] and PE included in TPP.[20] These observations are significant in that it is thus evidenced that the lateral motion of these molecules is rather slow. The strong distance dependence of the intensity build-up in such experiments ($\sim 1/r^6$ for homonuclear DQ correlation) means that on the time scale of a typical experiment, say 0.25 ms, the guest cannot move farther than about one host repeat unit (~5 Å). This constrains the diffusion coefficient associated with lateral motion to about 25 $Å^2/0.25$ ms $= 10^{-15}$ m^2/s as an upper limit.

While such slow lateral motion may not come as a surprise when polymers are considered, it is worthwhile to investigate the situation for shorter and more mobile alkanes. In the previous sections, we have already seen indirect evidence that guest−host couplings are nonnegligible. For a more detailed study, we have chosen homonuclear ^{1}H DQ MAS spectroscopy as an efficient tool. Figure 8 shows a 2D correlation spectrum, in which a well-developed cross-signal between guest and host can clearly be identified. Based on the above considerations, lateral diffusion is therefore also constrained to a rather low level.

In relatively full nanochannels, the characteristics of single-file diffusion have to be considered.[30,47] This special type of diffusion is encountered in one-dimensional systems, in which the diffusants cannot pass each other. On short time scales, local back and forth motions due to mutual collisions dominate, while on longer time scales, the mean-square displacement scales with $\sqrt{t}$, thus much more slowly than in regular diffusion, where $\langle \Delta z^2 \rangle \sim t$. The mobility factor associated with this sub-diffusive behavior depends strongly on loading. As typical self-diffusion constants of short alkanes in bulk are on the order of 10^{-10} m^2/s, we would expect similarly rapid local motions in the channels, as the interactions between the aromatic TPP channel structure and the alkanes are dominated by low-energy van der Waals contacts. Therefore, the observed guest−host dipolar coupling, reflected as a specific spectral intensity in the DQ experiment, should represent a fast-limit average over a length scale determined by the available lateral free volume, while an intensity loss at elevated temperatures should be additionally influenced by the loss of relative positional correlation related to motions following the $\sqrt{t}$ law.

In Figure 9, we have plotted the relative contribution of guest−host cross-signals to full DQ-filtered intensities, both

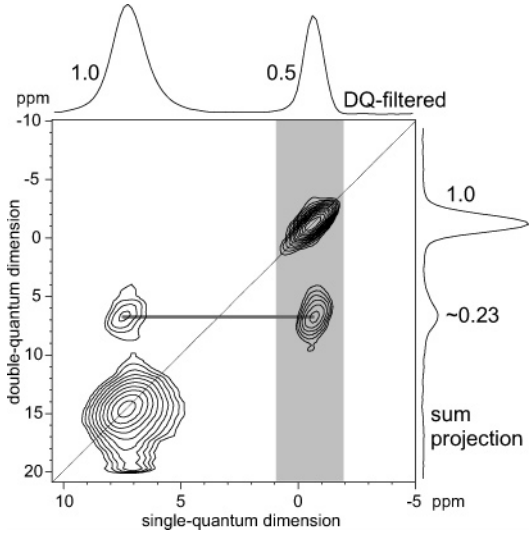

Figure 8. 2D DQ correlation spectrum of TPP−C9i at 30 kHz MAS and DQ excitation and reconversion times of 4 $\tau_R = 133.3$ μs each. Contours are spaced logarithmically, starting at 2% of the maximum intensity with an increment factor of 1.4. The projection along the DQ dimension is summed over the gray shaded area, and the horizontal bar indicates the guest−host dipolar contact.

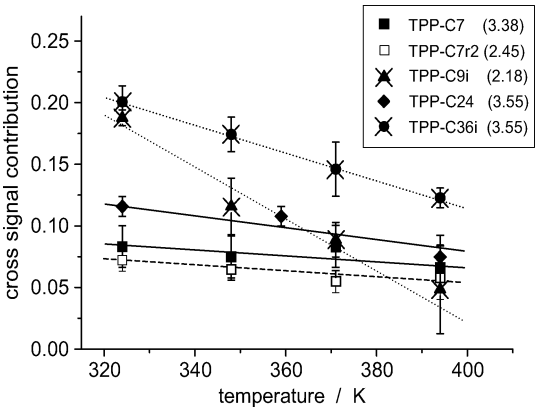

Figure 9. Intensity of the alkane-TPP cross signal detected at the alkane position in 2D DQ correlation spectra of TPP−ICs as a function of sample temperature, with experimental parameters given in the caption to Figure 8. The lines are guides to the eye, and crossed symbols again denote samples with impurities. The numbers in brackets are the filling in terms of CH_2 units per TPP molecule.

detected at the alkane resonance (see the sum projection in Figure 8). The latter quantity represents a viable intensity reference, as it is largely dominated by intraalkane dipolar couplings, which are practically constant over the investigated range of chain lengths and temperatures, as evidenced in the previous sections. The relative cross-signal intensity should therefore be a measure of the lateral free volume available in the channels. We observe that it is neither correlated directly with chain length, nor is it a strong function of temperature. Reassuringly yet, the cross signal intensity decreases with decreasing filling, in agreement with the discussion of the previous section: low filling leads to increased lateral free volume (as observed here), and thus to less frequent interalkane collisions (which introduce less gauche conformers).

An exception to the general trend is the aged samples, in which lateral mobility appears more highly activated. Yet again, the large cross-signal contributions at lower temperatures indicate decreased lateral free volume and therefore motivate the higher gauche contents found for these samples. This supports the notion that the alkanes tend to cluster in the intact

regions of the aged samples. We refrain from drawing further conclusions on the increased temperature dependence, since we have at present no additional evidence as to whether aging might also lead to more dynamic or less ordered channel structure, which could also comprise obstacles or open ends. The final explanation of the temperature dependence might involve a complex interplay of more than one of these factors.

IV. Summary and Conclusions

Two dipolar recoupling methods were used to study site-resolved, fast-motion-averaged $^{13}C-^{1}H$ dipolar couplings in alkanes of different length confined to nanochannels formed by TPP and urea matrices. REREDOR, a robust fast-MAS method working at 30 kHz spinning, provided support of the possibility to analyze the data in terms of isolated methylene and methyl groups without the need for calibration. Effects of couplings to remote channel protons were clearly present in the corresponding SLF-type dipolar sideband spectra, but mainly affected the intensity of the centerband. The level of perturbation was estimated to an order of 1−2 kHz when modeling a guest−host interaction by three symmetrically positioned remote protons. Intra-$CH_{2,3}$ couplings could still be obtained with good confidence, but only to a level of about 5% accuracy, this limitation being set by experimental noise due to the use of small 2.5 mm rotors and sample of natural isotopic abundance.

Much improved precision to about 1% was possible by measuring LG-CP build-up curves in 4 mm rotors at 11 kHz MAS, where we proposed an efficient protocol focusing on the analysis of extrema positions instead of acquiring full time domain data and obtaining dipolar spectra after Fourier transformation. Calibration functions relating extrema positions with dipolar coupling constants were derived on the basis of spin dynamics simulations. The quality of the setup can be monitored by using an internal reference, which was in our case provided by rigid CH groups of the TPP matrix.

Our results on urea-ICs were found to be fully consistent with recent literature, where deuterium splittings in labeled compounds were analyzed. For TPP, we identified a tendency toward lower order parameters than in urea, which is surprising considering its nominally lower channel diameter. The chain order was found to decrease toward the chain ends, as one would intuitively expect. For shorter included alkanes, the order parameters associated with the inner parts of the chains tend to vary over increasingly wide ranges, with the lowest values found for highly filled and aged samples. Similar trends were observed for the isotropic chemical shifts of the different chain carbons, also in accordance with earlier results on urea- and TPP-ICs. These variations were explained with increasing amounts of gauche conformers, where high filling leads to frequent collisions and consequently less ordered chains. Aging effects were attributed to clustering of the remaining alkane in the intact parts of the nanochannel structure.

Both dipolar couplings and chemical shifts were quantitatively analyzed in terms of simple models based on a small amount of $\{g_+-t-g_-\}$ conformers, which rapidly interconvert with an otherwise all-trans configuration. This leads to additional averaging of dipolar couplings due to different orientations of CH dipolar tensors on one hand, and to changes in the chemical shift due to the γ-gauche effect on the other hand. The results of both types of analysis, even though based on completely different effects, are consistent and indicate gauche contents ranging from about 13% for some heptane-ICs down to 2−3% for $C_{54}H_{110}$ at room temperature. Slightly lower order, thus higher gauche content, was indicated by experiments performed 40 K above room temperature, and more systematic studies should possibly reveal the relative energy of the gauche-containing channel conformers.

While the heteronuclear experiments provided first hints to nonnegligible guest−host dipolar contacts, more specific ^{1}H DQ correlation experiments gave direct evidence of guest−host interactions, which were previously observed only for included polymers. This observation led us to conclude that long-range lateral motions of the alkanes must be restricted to diffusion coefficients below 10^{-15} m^2/s. Rapid local back and forth motions resulting from interalkane collisions lead to an averaging of the guest−host interactions and must be restricted to the Å range.

The observed guest−host DQ intensities are a direct (inverse) measure of this lateral free volume, and as expected, lower loading leads to decreased intensities. The weak temperature dependence is attributed to the restrictions imposed by single-file diffusion as the only possible mechanism for long-range loss of correlation. Also in these experiments, aged samples were found to behave somewhat differently, in that the local motions exhibit a stronger temperature dependence and appear to be more constrained, possibly because the alkanes are expelled from the degraded channel structure and cluster more tightly in the intact parts.

Acknowledgment. Funding was provided by the Deutsche Forschungsgemeinschaft (SFB 428) and the Fonds der Chemischen Industrie. Klaus Müller is acknowledged for his generous gift of the urea-C16 compound, and Katharina Dixa for the synthesis of urea-C12. Heino Finkelmann is acknowledged for providing access to the 500 MHz spectrometer in Freiburg, where most of this work was conducted.

References and Notes

(1) Lu, J.; Mirau, P. A.; Tonelli, A. E. *Prog. Polym. Sci.* **2002**, *27*, 357−401.
(2) Schlenk, W. *Ann. Chem. J. Liebig* **1949**, *565*, 204−240.
(3) White, D. M. *J. Am. Chem. Soc.* **1960**, *82*, 5678−5685.
(4) Tonelli, A. E. *Polym. Int.* **1997**, *43*, 295−309.
(5) Wei, M.; Davis, W.; Urban, B.; Song, Y.; Porbeni, F. E.; Wang, X.; White, J. L.; Balik, C. M.; Rusa, C. C.; Fox, J.; Tonelli, A. E. *Macromolecules* **2002**, *35*, 8039−8044.
(6) Tonelli, A. E. *Macromolecules* **1990**, *23*, 3134−3137.
(7) Meirovitch, E.; Belski, I. *J. Phys. Chem.* **1984**, *88*, 6407−6411.
(8) Casal, H. L.; Cameron, D. G.; Kelusky, E. C. *J. Chem. Phys.* **1984**, *80*, 1407−1410.
(9) Imashiro, F.; Maeda, T.; Nakai, T.; Saika, A.; Terao, T. *J. Phys. Chem.* **1986**, *90*, 5498−5500.
(10) Imashiro, F.; Kuwahara, D.; Nakai, T.; Terao, T. *J. Chem. Phys.* **1989**, *90*, 3356−3362.
(11) Sozzani, P.; Bovey, F. A.; Schilling, F. C. *Macromolecules* **1989**, *22*, 4225−4230.
(12) Sozzani, P.; Bovey, F. A.; Schilling, F. C. *Macromolecules* **1991**, *24*, 6764−6768.
(13) Brückner, S.; Sozzani, P.; Boeffel, C.; Destri, S.; Di Silvestro, G. *Macromolecules* **1989**, *22*, 607−611.
(14) Sozzani, P.; Behling, R. W.; Schilling, F. C.; Brückner, S.; Helfland, E.; Bovey, F. A.; Jelinski, L. W. *Macromolecules* **1989**, *22*, 3318−3322.
(15) Schilling, F. C.; Amundson, K. R.; Sozzani, P. *Macromolecules* **1994**, *27*, 6498−6502.
(16) Cannarozzi, G. M.; Meresi, G. H.; Vold, R. L.; Vold, R. R. *J. Phys. Chem.* **1991**, *95*, 1525−1527.
(17) Schmider, J.; Müller, K. *J. Phys. Chem. A* **1998**, *102*, 1181−1193.
(18) Comotti, A. Simonutti, R.; Catel, G.; Sozzani, P. *Chem. Mater.* **1999**, *11*, 1476−1483.
(19) Saalwächter, K. *Macromol. Rapid Commun.* **2002**, *23*, 286−291.
(20) Sozzani, P.; Comotti, A.; Bracco, S.; Simonutti, R. *Chem. Commun.* **2004**, 768−769.
(21) Schmidt-Rohr, K.; Spiess, H. W. *Multidimensional Solid-State NMR and Polymers*; Academic Press: London, 1994.
(22) Tonelli, A. E. *NMR Spectroscopy and Polymer Microstructure: The Conformational Connection*; VCH: Weinheim, 1989.

(23) Terao, T.; Miura, H.; Saika, A. *J. Chem. Phys.* **1986**, *85*, 3816−3826.
(24) Dusold, S.; Sebald, A. *Ann. Rep. NMR Spectrosc.* **2000**, *41*, 185−262.
(25) Saalwächter, K.; Graf, R.; Spiess, H. W. *J. Magn. Reson.* **1999**, *140*, 471−476.
(26) van Rossum, B.-J.; de Groot, C. P.; Ladizhansky, V.; Vega, S.; de Groot, H. J. M. *J. Am. Chem. Soc.* **2000**, *122*, 3465−3472.
(27) Saalwächter, K.; Graf, R.; Spiess, H. W. *J. Magn. Reson.* **2001**, *148*, 398−418.
(28) Saalwächter, K.; Schnell, I. *Solid State Nucl. Magn. Reson.* **2002**, *22*, 154−187.
(29) Allcock, H. R.; Siegel, L. A. *J. Am. Chem. Soc.* **1964**, *86*, 5140−5144.
(30) Meersmann, T.; Logan, J. W.; Simonutti, R.; Caldarelli, S.; Comotti, A.; Sozzani, P.; Kaiser, L. G.; Pines, A. *J. Phys. Chem. A* **2000**, *104*, 11665−11670.
(31) van Moorsel, G.-J. M. P.; van Eck, E. R. H.; Grey, C. P. *J. Magn. Reson. A* **1995**, *113*, 159−163.
(32) Gullion, T.; Schaefer, J. *J. Magn. Reson.* **1989**, *81*, 196−200.
(33) Bennett, A. E.; Rienstra, C. M.; Auger, M.; Lakshmi, K. V.; Griffin, R. G. *J. Chem. Phys.* **1995**, *103*, 6951−6958.
(34) Metz, G.; Wu, X.; Smith, S. O. *J. Magn. Reson. A* **1994**, *110*, 219−227.
(35) Ernst, R. R.; Bodenhausen, G.; Wokaun, A. *Principles of Nuclear Magnetic Resonance in One and Two Dimensions*; Clarendon Press: Oxford, 1987.
(36) Graf, R.; Demco, D. E.; Gottwald, J.; Hafner, S.; Spiess, H. W. *J. Chem. Phys.* **1997**, *106*, 885−895.
(37) Feike, M.; Demco, D. E.; Graf, R.; Gottwald, J.; Hafner, S.; Spiess, H. W. *J. Magn. Reson. A* **1996**, *122*, 214−221.
(38) Bak, M.; Rasmussen, J. T.; Nielsen, N. C. *J. Magn. Reson.* **2000**, *147*, 296−330.
(39) Bak, M.; Nielsen, N. C. *J. Magn. Reson.* **1997**, *125*, 132−139.
(40) Hester, R. K.; Ackerman, J. L.; Neff, B. L.; Waugh, J. W. *Phys. Rev. Lett.* **1976**, *36*, 1081−1083.
(41) Hong, M.; Yao, X.; Jakes, K.; Huster, D. *J. Phys. Chem. B* **2002**, *106*, 7355−7364.
(42) Lee, M.; Goldburg, W. I. *Phys. Rev. A* **1965**, *140*, 1261−1271.
(43) Simonutti, R.; Mauri, M.; Bracco, S.; Comotti, A.; Sozzani, P. *Polym. Prepr.* **2003**, *44*, 361−362.
(44) Hentschel, D.; Sillescu, H.; Spiess, H. W. *Makromol. Chem.* **1979**, *180*, 241−249.
(45) Zerbi, G.; Longhi, G. *Polymer* **1988**, *29*, 1827−1830.
(46) Odin, C.; Ameline, J. C. *Europhys. Lett.* **2004**, *66*, 378−384.
(47) Hahn, K.; Kärger, J.; Kukla, V. *Phys. Rev. Lett.* **1996**, *76*, 2762−2765.